Sādhanā Vol. 38, Part 2, April 2013, pp. 247–264. © Indian Academy of Sciences

An experimental stationary quadrotor with variable DOF

VASFI EMRE ÖMÜRLÜ[1], UTKU BÜYÜKŞAHIN[1],
REMZI ARTAR[2], AHMET KIRLI[1] and M NURULLAH TURGUT[1]

[1]Mechatronic Engineering Department, Yildiz Technical University,
Istanbul 34349, Turkey
[2]Mechanical Engineering Department, Istanbul Technical University,
Istanbul 34469, Turkey
e-mail: omurlu@yildiz.edu.tr; buyuksah@yildiz.edu.tr;
remzi.artar@simcotech.com.tr; akirli@yildiz.edu.tr; mturgut@yildiz.edu.tr

MS received 11 August 2010; revised 28 November 2011; accepted 7 February 2013

Abstract. Unmanned air vehicles (UAV) and especially quadrotors have drawn great attention in recent years because of their maneuverability, ease of design and control. Most of the works concentrate mostly on control; yet, design and communication are also some sub-topics. In this research, a stationary, four rotor air vehicle with limited/controlled degree of freedom is constructed so that various control algorithms and their changing effects with varying vehicle dynamics can be studied on the ground for safety purposes. Ascending/descending, pitch/yaw/roll motions can be limited/controlled by setting the vehicle's degree of freedom mechanically, resulting better net observability of the control algorithms on the vehicle's dynamic performance. Design, in terms of mechanics, mechatronics and software is presented and the usability of the system is shown. Parallel self tuning fuzzy PD + PD control is applied to the system for preliminary studies and results are discussed. Inspite of the sensor noise, satisfactory pitch/roll/yaw control is achieved.

Keywords. UAV; Quadrotor; fuzzy control; matlab embedded function.

1. Introduction

Since the time of Leonardo da Vinci, continuous research and developments are made about helicopters. Being a sub-class of helicopters, quadrotors attract special attention in recent years for which real time speed control of the motors is required for navigation. Continuous variation of the rotor speeds affect the vertical thrust and this coupled dynamics triggers the navigational control problem. For instance, Hoffmann *et al* (2004) presented a miniaturized air vehicle which follows a pre-defined path where disturbances affect the elevation depending on continuously varying motor speeds. Altug *et al* (2002) employed camera feedback as a main sensor and a motion/position feedback device controlling a four rotor air vehicle. Pounds *et al* (2002) used indoor four rotor air robot, X4 Flyer model, in their study and presented the satisfactory results of the internal loop controller. Fang *et al* (2008) aimed to control the translational position and yaw

angle of a quadrotor in simulation by employing new continuous sliding mode control, based on feedback linearization. Raffo *et al* (2010) presented a control scheme for a quadrotor based on model predictive control for path following and nonlinear H^{∞} controller for rotational stabilization. Another type of control algorithm based on neural networks was presented in Dierks & Jagannathan (2010) in which NN is introduced to learn about the dynamics including aerodynamic friction and blade flapping. Efe (2007) referred to a dynamic model of a Dragonfly quadrotor, where he applied nonlinear control and presented its performance and motion characteristics. Some other control topics that have been studied extensively on UAVs in simulation environment are presented in Mokhtari *et al* (2006) and Castillo *et al* (2005). Additionally, modelling using Newton–Euler method and following sequential nonlinear control strategy was developed in Mian & Daobo (2008) in which feedback linearization coupled with a PD controller for translational motion and backstepping based PID nonlinear controller for rotational stability was employed. Kim *et al* (2010) presented a disturbance observer after managing a rigorous modelling with respect to both earth and body frame and claimed to have a successful hovering control of a quadrotor. Alternatively, momentum theory for modelling of a quadrotor was used in Amir & Abbass (2008) neglecting gyroscopic effects and air friction resulting in a simplified model which was used to stabilize the vehicle in hovering state.

It would be wise to extend control studies of air vehicles on a stationary unit or in simulation environment because of the possibility of injuries during trials. Thus, several experimental stationary four rotor air vehicles with various capabilities have been constructed. For example, Ömürlü *et al* (2011) presented a multi degree of freedom experimental set-up for controller design purposes by avoiding injuries and Bouabdallah *et al* (2004) aimed to study pitch/yaw/roll control on an experimental OS4 autonomous robot when the motion in vertical direction was kept constant. Baran *et al* (2008) experimented various control algorithms for UAVs on a six degree of freedom (DOF) stationary test system. Pongpaibul (2001) studied on a computer controlled mini flying vehicle and performed vertical motion stabilization and motion control experiments on a two-propeller test system. Patel *et al* (2006) designed a Dragonfly-based test system with safeguard frame. Some investigations as in Tayebi & McGilvray (2006) consisted of four rotor test systems with only elevation control stabilization placed on a spherical joint. Another six DOF quadrotor test system was obtained by placing the air vehicle on a shaft on which two universal joints were placed at both ends as presented in Chen & Huzmezan (2003).

In this study, various aspects of a stationary experimental quadrotor system with variable degree of freedom are discussed. Mechanic design, mechatronic design issues and digital signal controller based control system are explained in section 2. After the explanation of pre-calibration of the motors and of the sensors, section 3 briefly introduces the well-known dynamic model of the air vehicle. Section 4 presents the control algorithms employed for preliminary control studies and the response of the stationary vehicle is shown and discussed in section 5.

2. Four rotor air vehicle flight control unit

Mechanic, mechatronic and software are the main concerns of the intended unit. Mechanics aim to decouple different motion axis of the vehicle so that control algorithm effects can be observed. While mechatronic design searches for the best combination of the system control components, software stage optimizes processing time.

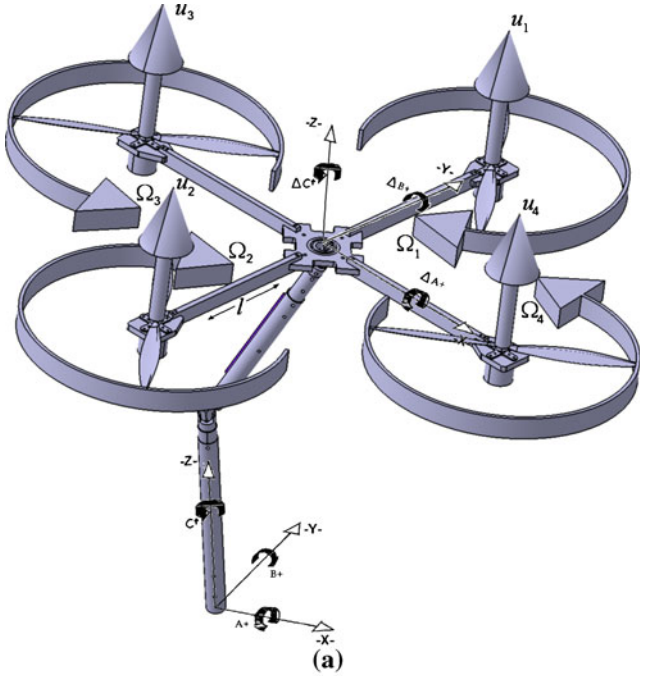

Figure 1. (**a**) Variables, coordinate system and the general structure of a quadrotor system. (**b**) A stationary flight control system with variable degree of freedom for unmanned four rotor air vehicles.

2.1 *Mechanical design*

The mobility of the vehicle is intended to be set variably to observe the effect of control algorithms for different axes as in figure 1b. Elevation, yaw, pitch/roll or full DOF can be controlled separately as shown in figure 2. Rotations around x, y and z axis are called pitch, roll and yaw, respectively. A roller bearing and a universal joint are used in mechanical design to obtain this mobility. Universal joint allows the pitch/roll rotations while the roller bearing lets yaw rotation which reduces the rotational friction extensively providing near-flight dynamics. While pitch/roll motion can be limited partly or fully by placing a ring around the universal joint as in figure 2c, yaw motion can be restricted by locking screws affecting the bearing as in figure 2b.

A second universal joint is placed between two shafts connected in series carrying the quadrocopter which allows spatial motion of the vehicle after 20 cm lift as presented in figure 2d. A lock is placed on the system so that shafts and the vehicle cannot exceed 80 cm elevation. Additionally, pitch/roll motion is limited with 45°, yet this limit is disabled after spatial motion is enabled after 20 cm lift.

2.2 *Mechatronic design*

Figure 3 shows the system elements and the connection between them. TMS320F28335 digital signal controller of TI is chosen as a main processor because of its processing and DAC speed, variety of peripherals and related Matlab/Simulink interface. Pitch/roll angles are sensed by

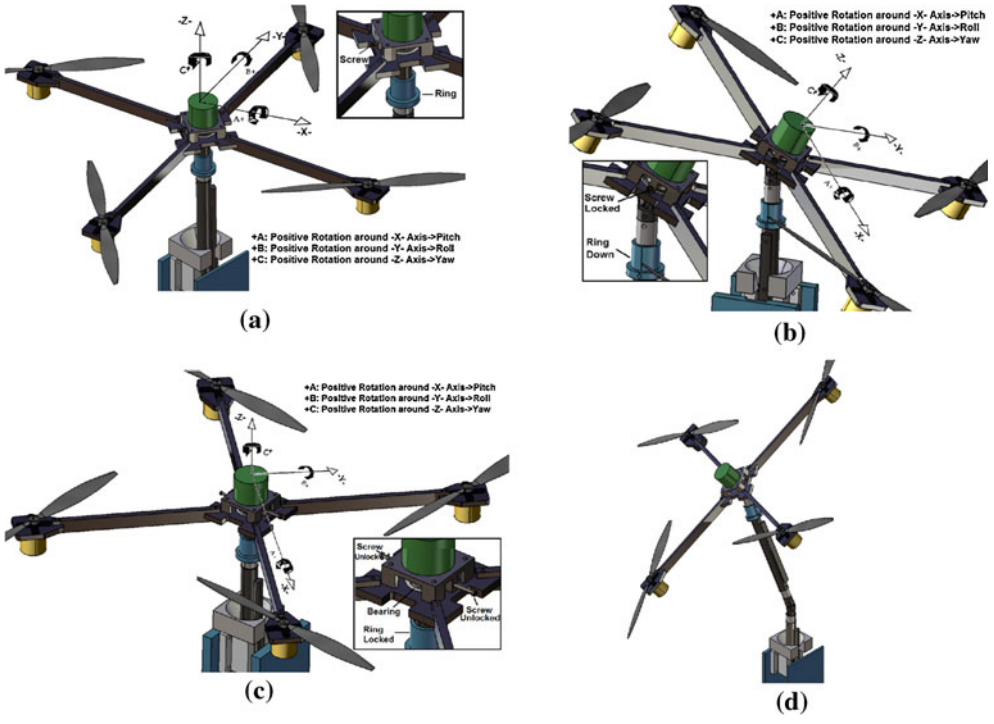

Figure 2. (**a**) Vertical elevation control while locking rings for pitch/yaw/roll motion in place. (**b**) Pitch/Roll control while locking screw for yaw motion in place. (**c**) Yaw control while locking rings for pitch/roll motion in place. (**d**) Spatial motion of the quadrotor in the stationary testbed.

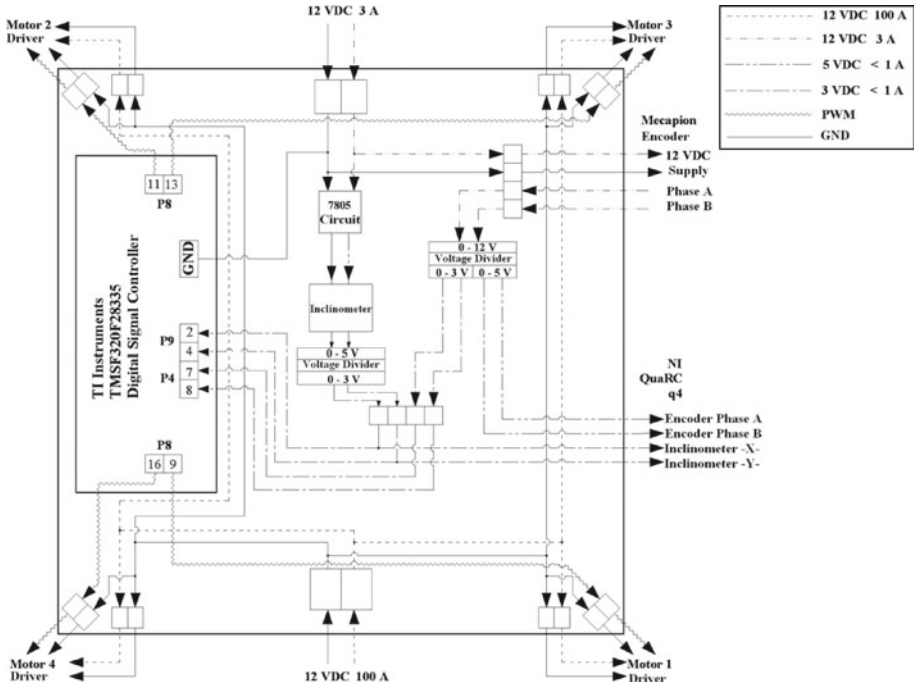

Figure 3. Control board schematics.

SCA100 T-D02 inclinometer and 12 bit DAC with 80 ns reading time converts the angles with resolution of 0.0025 degrees and 10 Hz bandwidth. Since employed Hacker X40 DC servo motor drivers accept PWM inputs of 10–20% duty cycles and generates 0–18000 rpm of corresponding speed, PWM resolution is crucial for speed control. In order to control motor speeds with sufficient resolution, PWM modules are pre-conditioned for which initial PWM duty cycle is kept at 4% and processor main timer is divided to $8 \times 4 = 32$. Thus, PWM duty cycle is able to be divided in to 46900 which corresponds to the speed resolution of 3.84 rpm.

Since there appears to be four controllable axes for quadrotors, they have four DOF, although they perform spatial motion and seem like six DOF vehicles. That is because rotation around x axis and translation along y axis and also, rotation around y axis and translation along x axis are coupled. Eventually, controllable motions are rotations around x, y and z axes and elevation along z axis. Thus, related sensors are selected for feedback purposes. Pre-mentioned SCA100T-D02 inclinometer can measure the inclination by 0.0025 degrees resolution. Taking advantage of being stationary, 2000 line rotary encoder with TTL output is employed to read rotation around z axis, yaw motion. Also, linear encoder of 0.1 mm resolution is used to measure the motion along z axis, elevation. Naturally, last two types of encoders are not logical to be used on a flying UAV, yet stationary and precision sensors are preferred because of the intended mobility-dependent control algorithm.

LiPo (Lithium-Polymer) batteries are the ones that are mostly used on air vehicles as power sources because of their high power/weight ratio. However, uptime of LiPo batteries is short and their charging time is pretty long. Thus, 100 A varying and 12 V constant stationary DC power is preferred to provide power to the motor drivers. Also, a 3 A varying and 12 V constant stationary DC power is used to provide power to *electronic* equipment.

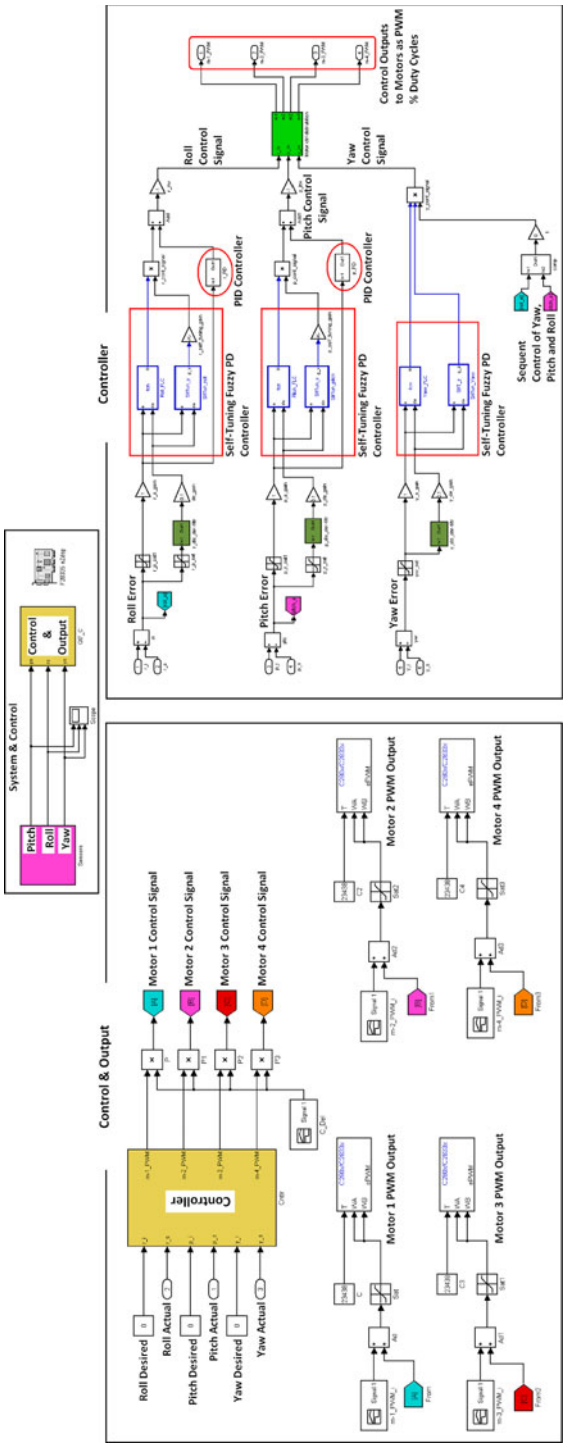

Figure 4. Matlab–Simulink interface of the control system.

2.3 *Control interface*

As it has been mentioned, system is interfaced and controlled by a TMS320F28335 digital signal controller programmed through the starter kit of the same processor. Control and input/output management are performed through Matlab-Simulink blocks of the processor as shown in figure 4. Although access to full processor functions is available from Simulink blocks, slight excess use of these blocks increases the memory usage drastically. Especially, since fuzzy control design is intended in this study, availability of fuzzy design tools is a must through FIS fuzzy design tool of Simulink. However, usage of a single FIS block in Simulink increases the processor memory usage considerably, when compiling is performed. Therefore, fuzzy sets of self tuning sections of the controllers which consist of pitch, roll and yaw control, are directly programmed through Matlab Embedded Function blocks for the sake of using less processor memory.

Controller inputs of the excitation system are the desired angles of roll, pitch, yaw and the actual angles of roll, pitch, yaw which are obtained by the rotary encoder and the inclinometer. Since high resolution analog inclinometer sensor is easily affected by environmental noises, IIR Butterworth low pass filters are used for filtering purposes. Since the drivers are to be pre-actuated below 10% PWM duty cycle, motor initial values are set to 8% duty cycle. Since error signals, the derivative of errors and the control signals are all limited to the calculated and predetermined values, some saturation blocks are employed. The control signal of the motors is %PWM duty cycle, so the limitation for the control signal is 10 to 20. The controller is designed to perform the control at around 15% duty cycle which provides necessary power to hold the quadrocopter on the air.

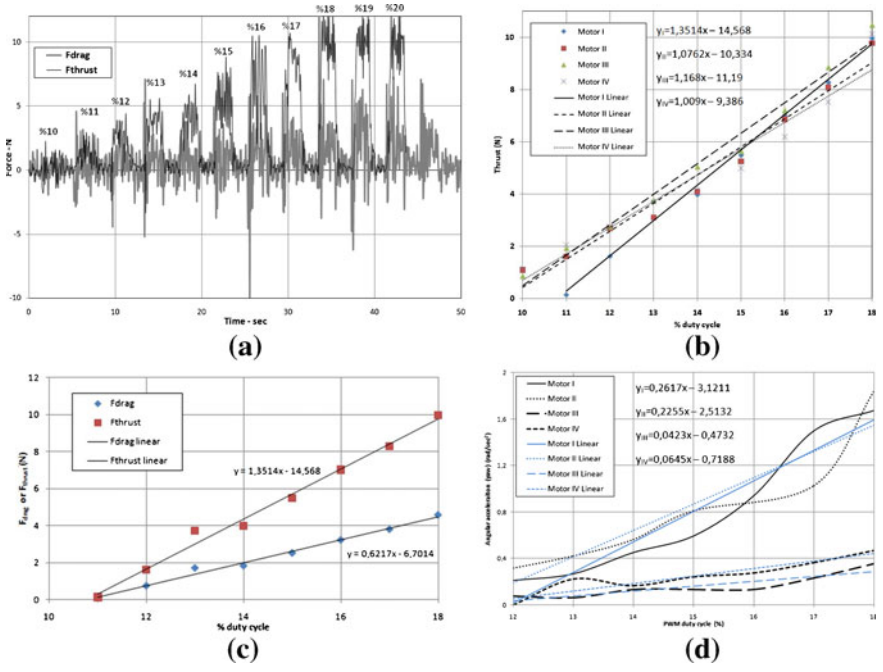

Figure 5. (**a**) Drag and thrust force outputs of motor I for several PWM % duty cycles. (**b**) Static thrust of the motors for increasing PWM % duty cycle for selecting motor pairs. (**c**) Motor I thrust and drag relationship. (**d**) Max yaw accelerations based on motor input PWM percent duty cycles.

Since each of four motors have slight differences in thrust and drag forces, these variations are embedded into the control system as compensation and initial calibration of the system as in figure 5b. By this way, it is ensured that control design only compensates for the required directional inputs.

2.4 *Pre-calibration of excitation system*

2.4a *Motors*: Although the motors are assumed to be exact, internal performance and parameter variations cause different characteristics in thrust as presented in figure 5b, and in resultant drag values as in figure 5a. Figure 5a represents the motor-I thrust and drag values for changing input PWM duty cycles. Additionally, figure 5b shows the corresponding motor thrust for given PWM duty cycle inputs. Thrust variations of the motors depending on input PWM varies among motors slightly. Therefore, facing motors are chosen to create better balancing condition of the air vehicle. That is, motor I–III and motor II–IV are selected to be the facing pairs because of their near-exact matching thrust characteristics.

The graph of thrust forces of all four motors responding to the step inputs from 10% to 20% duty cycle that are responsible for the elevation of the vehicle is in figure 5a. The sampling time of the system is 1 ms which means that the control loop runs at 1 kHz. The minimum value of the PWM % duty cycle is determined, so as to keep the total vertical thrust, about more than the structural weight.

Figure 5c shows the relationship between thrust and drag forces of motor I for which the ratio between these forces is experimentally proven to be around 0.46. Since numerical relationship is found, other drag forces can be calculated using this value. The mathematical proof of this ratio is also performed, that is, the area of side and vertical sweep of the propeller used is found to be 0.46.

Since yaw control of the system depends on the torque generated by drag forces of each motor, effects of both drag forces and connection cables on the dynamics should be considered. Thus, time-response-based yaw accelerations depending on motor input duty cycles are studied extensively for related motor output adjustments as shown in figure 5d. Since rotational acceleration provided by each motor obtained from their time response is different, yaw control inputs to the motors are pre-calibrated by balancing the motor effects around yaw axis. This will ensure the homogenous control effect generated by each motor.

2.4b *Sensors - inclinometer*: It is mentioned that SCA100T-D02 inclinometer can measure pitch/roll angles by 0.0025 degrees resolution, yet this resolution is available at the analog output of the inclinometer. This analog signal is connected to the TMS320F28335 microcontroller which has 12 bit ADC resolution. The resolution for the feedback is calculated as $180/(2\hat{}12) = 0.044$ degrees. The dual axes inclinometer produces 0 to 5 volts for varying angles from -90 to $+90$ degrees and 2.5 volts is the output when the inclinometer is parallel to the ground. In other words, -90 degrees is 0 volts, 0 degrees is 2.5 volts and 90 degrees is 5 volts. Besides the drawback caused by the ADC resolution of the DSC employed, environmental noises should be considered as can be seen in figure 6a. The average of the noise magnitude is approximately 0.5 degrees which would be ignored, yet the peaks are approximately 1.5 degrees which has a considerable effect on the control. Since the inclinometer employs accelerometers, in order to minimize the errors of the analog sensor, a low pass filter is designed as shown in figure 6b in which the inclination angle varies when the acceleration is high and also there is a constant

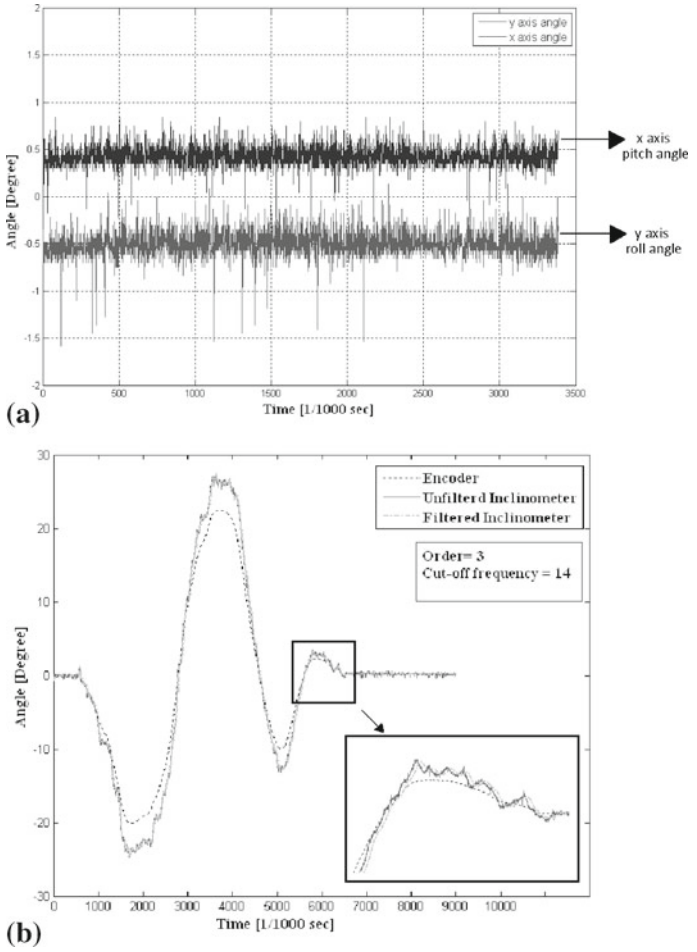

Figure 6. (**a**) Noise observed at the output of the inclinometer when it is parallel to the ground. (**b**) Filtered and unfiltered inclinometer's comparison.

oscillating error. In this figure, the encoder shows the absolute angle of inclination. Additionally, the high frequency of the noise variations generates other problems for the control system which include the derivative term of the error.

3. Mathematical model

A quadrotor, four rotor air vehicle, has vertical motion and hovering capability with its four motors and can navigate in space by varying and controlling the motor speeds. Since the neighbouring wings have reverse helical angles, there is no need for a balancing tail rotor which is necessary in helicopters to cancel the torsion created by the main propellers. Therefore, equal rotor speeds create ascending/descending motion. For example, keeping the 1st and 3rd motors at the same speed, a quadrotor will move along x axis for different speeds of 2nd and 4th rotors. Additionally, the air vehicle will move along y axis for different speeds of 1st and 3rd motors

when 2nd and 4th propeller speeds are kept the same. A quadrotor has the ability to rotate around its vertical axis when moving along back and forth and side to side.

Dynamic model of the system can be obtained by using Newton Euler model as the earth inertial frame (E-Frame) $\dot{\xi} = \left[\dot{X}\ \dot{Y}\ \dot{Z}\ \dot{\phi}\ \dot{\theta}\ \dot{\psi}\right]^T$, and the body-fixed frame (B Frame), $\boldsymbol{v} = [u\ \ v\ \ w\ \ p\ \ q\ \ r]^T$ where $\dot{\xi}$ is the generalized velocity vector of E-frame, $\boldsymbol{v}$ is the generalized velocity vector of B-frame. Because of the time-independent inertia matrix, of body-symmetry-related simplified equations and of having the lifting forces directly on the B-frame, dynamics of the system can be formulated with respect to B-frame. However, since elevation and directional controls are needed with respect to E-frame, it is easy to express the dynamics of the control as a hybrid system called H-frame by composing linear equations of E-Frame and angular equations of B-frame $\varsigma = \left[\dot{X}\ \dot{Y}\ \dot{Z}\ \ p\ \ q\ \ r\right]^T$ as given in Bresciani (2008). As a result, kinematics of a generic 6 DOF rigid-body can be expressed as $\dot{\xi} = J_{\Theta} v$. Whole system of equations can be shown as

$$\ddot{X} = \left(S_\phi S_\psi + C_\phi C_\psi S_\theta\right) \cdot U_1 / m \tag{1}$$

$$\ddot{Y} = \left(-S_\phi C_\psi + C_\phi S_\psi S_\theta\right) \cdot U_1 / m \tag{2}$$

$$\ddot{Z} = -g + \left(C_\phi C_\theta\right) \cdot U_1 / m \tag{3}$$

$$\ddot{\phi} = \frac{I_{yy} - I_{zz}}{I_{xx}} \cdot \dot{\psi} \cdot \dot{\theta} \cdot - \frac{J_{TP}}{I_{xx}} \cdot \dot{\theta} \cdot \Omega + \frac{U_2}{I_{xx}} \tag{4}$$

$$\ddot{\theta} = \frac{I_{zz} - I_{xx}}{I_{yy}} \cdot \dot{\phi} \cdot \dot{\psi} + \frac{J_{TP}}{I_{yy}} \cdot \dot{\phi} \cdot \Omega + \frac{U_3}{I_{yy}} \tag{5}$$

$$\ddot{\psi} = \frac{I_{xx} - I_{yy}}{I_{zz}} \cdot \dot{\theta} \cdot \dot{\phi} + \frac{U_4}{I_{zz}} \tag{6}$$

$$U_1 = b \cdot \left(\Omega_1^2 + \Omega_2^2 + \Omega_3^2 + \Omega_4^2\right) \tag{7}$$

$$U_2 = l \cdot b \cdot \left(-\Omega_2^2 + \Omega_4^2\right) \tag{8}$$

$$U_3 = l \cdot b \cdot \left(-\Omega_1^2 + \Omega_3^2\right) \tag{9}$$

$$U_4 = d \cdot \left(-\Omega_1^2 + \Omega_2^2 - \Omega_3^2 + \Omega_4^2\right) \tag{10}$$

$$\Omega = -\Omega_1 + \Omega_2 - \Omega_3 + \Omega_4. \tag{11}$$

Here, S and C, are sin and cos with angular values as sub indices respectively. U_1 is the actuated lift force on z axis, U_2, U_3 and U_4 are the torques around y, x and z axis, respectively. Ω is the total speed of propellers, J_{TP} is the total inertia with respect to propeller axis, I_{xx}, I_{yy} and I_{zz} are the inertia of the quadrotor around x, y and z axis. b is the thrust and d is the drag factor of the propellers.

4. Control algorithms

Although relatively simple PD controller is initially designed and experimented successfully for the yaw motion, this controller fails for pitch/roll axis because of the coupled dynamics of pitch/roll/yaw axes. A quadrotor has nonlinear dynamics and sensory feedbacks for pitch/roll motion are very noisy as mentioned. Despite the fact that a simple PD control or an FLC by itself can achieve the control theoretically, a parallel self tuning fuzzy PD + PD controller is designed for the quadrotor test system, experimentally.

4.1 *Comparison and design of the controller*

The theoretical model of the quadrotor does not include the motor dynamics and the mechanical frictions. Therefore the controller which is designed virtually by employing the mathematical model of the system using Simulink and Matlab cannot be applied on the experimental set-up directly in order to achieve a robust and successful implementation of the control on the real system, more sophisticated algorithms with flexibility and compensation ability are applied instead of classical PI or PID controller. Experimental works have shown that a controller with slower responses is better than a faster one because of the feedback noise and motors' time delay/response time. Performing numerous experiments on the self tuning Fuzzy PD with a parallel PID controller is constructed since a classical PI or PID controller cannot control the setup by itself as well as the Fuzzy PD. Parallel usage of these two controllers enable smooth and stable performance of the experimental systems. The selection of the controller values numerically are performed by trial and error yet but the initial values are chosen using Mudi & Pal (1999) and by applying Ziegler–Nichols method.

4.2 *Fuzzy PD controller*

To avoid the oscillatory effect of integral action in the system dynamics because of the dynamic relationship between rotation about x/y/z axis and the excitation torque on these axes, fuzzy-supported PD controller is used for the controller trials, figure 8a, and rule base is constructed as described in Mudi & Pal (1999). Proportional + derivative control is described as

$$U^{PD} = k_p \cdot e + k_d \cdot \dot{e} \tag{12}$$

where e and $\dot{e}$ can be selected as fuzzy variables. Eq. (12) describes the controller. Relationship between the coefficients of Fuzzy PD and PD controllers based on figure 7 can be written as

$$k_p = g_a \cdot F\{g_e\} \tag{13}$$

$$k_D = g_a \cdot F\{g_{de}\} \tag{14}$$

Then, controller output becomes,

$$U^{PD} = g_a \cdot \left[F\{g_e\} \cdot e + F\{g_{de}\} \cdot \dot{e}\right] \tag{15}$$

Table 1 lists the fuzzy rule base, where NB is negative big, NM is negative medium, NS is negative small, Z is zero, PS is positive small, PM is positive medium and PB is positive big.

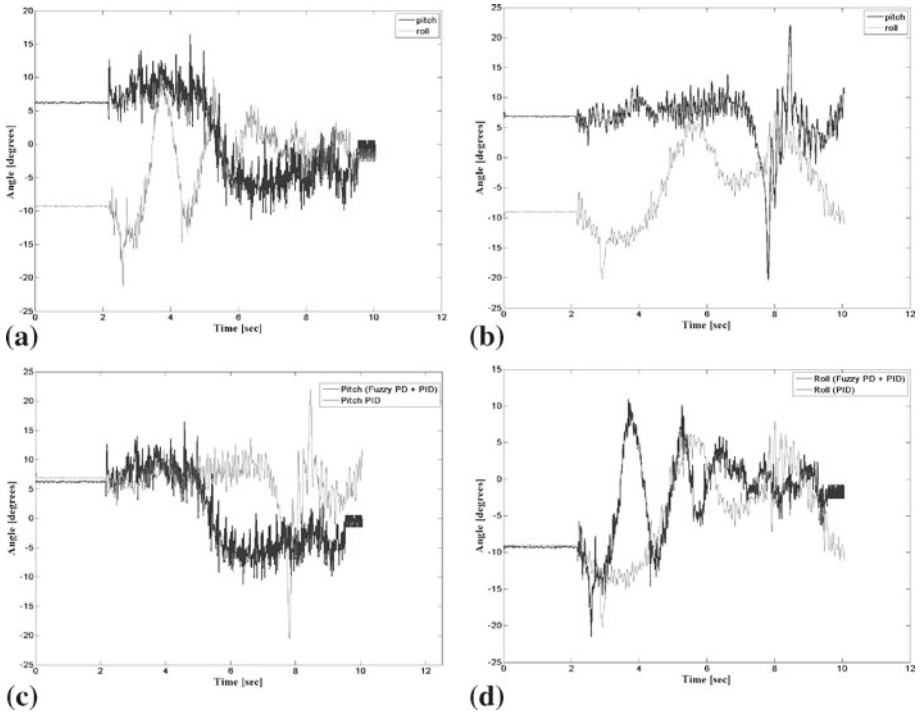

Figure 7. (**a**) Fuzzy PD + PID Control of the System. (**b**) PID Control of the System. (**c**) Fuzzy PD + PID and PID Control of Pitch. (**d**) Fuzzy PD + PID and PID Control of Roll.

4.3 *Self-tuning fuzzy PD controller*

Above-mentioned fuzzy PD controller may adjust its derivative effect real time, by placing a parallel self-tuning fuzzy rule base which adjusts the ga parameter, figure 8. This self-tuning effect can be represented as

$$U_{c1} = U^{PD} \cdot \underbrace{F\{e, \dot{e}\}}_{a} \tag{16}$$

Table 1. Rule base for fuzzy PD controller part.

Δe/e	NB	NM	NS	Z	PS	PM	PB
NB	NB	NB	NB	NM	NS	NS	Z
NM	NB	NM	NM	NM	NS	Z	PS
NS	NB	NM	NS	NS	Z	PS	PM
Z	NB	NM	NS	Z	PS	PM	PB
PS	NM	NS	Z	PS	PS	PM	PB
PM	NS	Z	PS	PM	PM	PM	PB
PB	Z	PS	PS	PM	PB	PB	PB

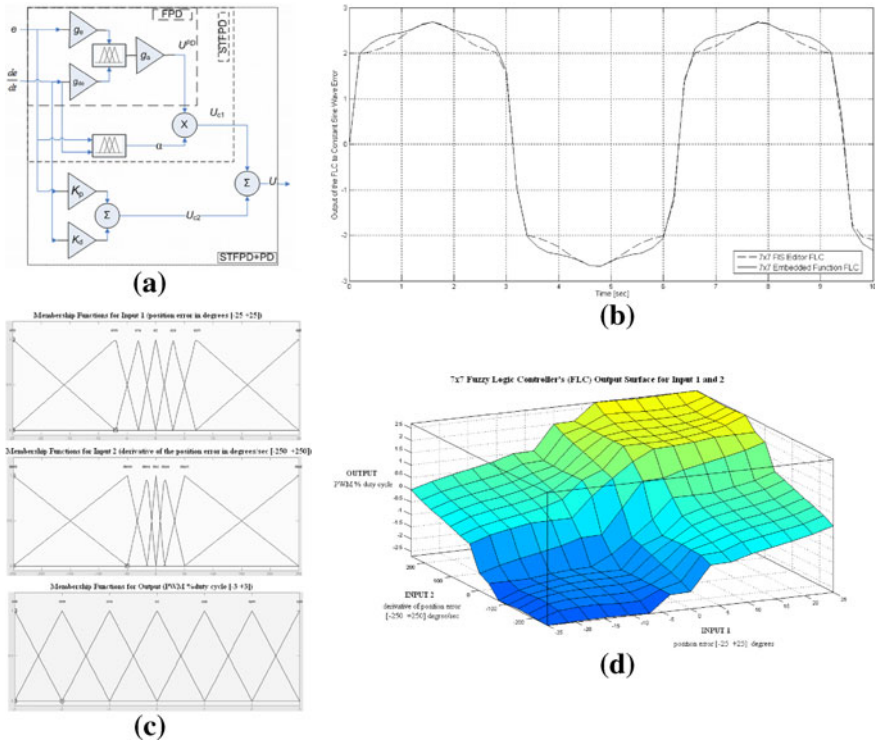

Figure 8. (**a**) Block diagram of the control algorithms. (**b**) Output of the 7 × 7 FIS Editor FLC and of the 7 × 7 embedded function FLC. (**c**) FLC Membership Functions. (**d**) 7 × 7 Fuzzy logic controller's (FLC) output surface for input 1 and 2.

U^{PD} is fuzzy PD output which is given by Eq. (12) and is multiplied by a parallel rule base, table 2, which depends on e and $\dot{e}$ where VB is very big, MB is medium big, B is big, Z is zero, S is small, MS is medium small, and VS is very small.

4.4 *Parallel self-tuning fuzzy PD controller*

In order to obtain better controller performance, a classic PD controller is placed parallel to the self-tuning fuzzy PD controller in which rule bases used are same as in tables 1 and 2

Table 2. Rule base for fuzzy self tuning part.

Δe/e	NB	NM	NS	Z	PS	PM	PB
NB	VB	VB	VB	B	SB	S	Z
NM	VB	VB	B	B	MB	S	VS
NS	VB	MB	B	VB	VS	S	VS
Z	S	SB	MB	Z	MB	SB	S
PS	VS	S	VS	VB	B	MB	VB
PM	VS	S	MB	B	B	VB	VB
PB	Z	S	SB	B	VB	VB	VB

presented in Han-Xiong & Gatland (1996) and Engin *et al* (2004). Controller output can be written as

$$U = K_p \cdot e + K_D \cdot \dot{e} + U^{PD} \cdot F\{e, \dot{e}\} \tag{17}$$

4.5 *Code-based fuzzy logic controller*

Because of the memory allocation problems of the TMS320F28335 microcontroller as mentioned in Control Interface section, FIS editor of the Matlab Software cannot be used for embedding into the DSC. Instead FLC (Fuzzy Logic Controller) are designed by using Matlab Embedded Function blocks in which the controller is directly written in c-code. Figure 8 represents the FLC's membership functions and the comparison of the output of the 7 × 7 FIS Editor FLC and output of the 7 × 7 Embedded Functions FLC for a constant sine wave error.

4.6 *Definitions of the FLC's membership functions*

The parameters that are required to design an FLC such as membership functions are defined as given above. For 7 × 7 FLC, 7 boundary definitions exist such as positive big, positive medium, positive small, zero, negative big, negative medium, negative small. The mathematical values of these parameters are decided experimentally as represented in figure 8c. Rule bases are designed as given in tables 1 and 2 and the surface of the FLC is formed as figure 8d. As mentioned in precalibration chapter, four DC servo motors are located on the system considering the variations in their dynamic behaviours. Similarly, output of the FLC is limited to ± 3V and this control signal is added to a constant, 13, which is the FLC's output. After the implementation of the PID controller's output, it becomes the overall control signal for the motor drivers in PWM% duty cycle unit.

5. Results

Response of the system to a series of inputs to check the control effectiveness is collected. Since dynamic coupling between pitch-roll and yaw motion exists and pitch-roll compensation affects

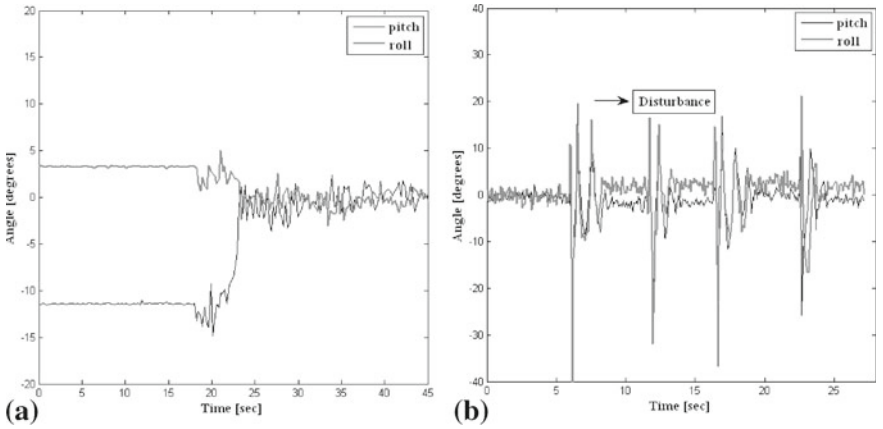

Figure 9. (**a**) System response to an initial condition. (**b**) System response to random disturbances.

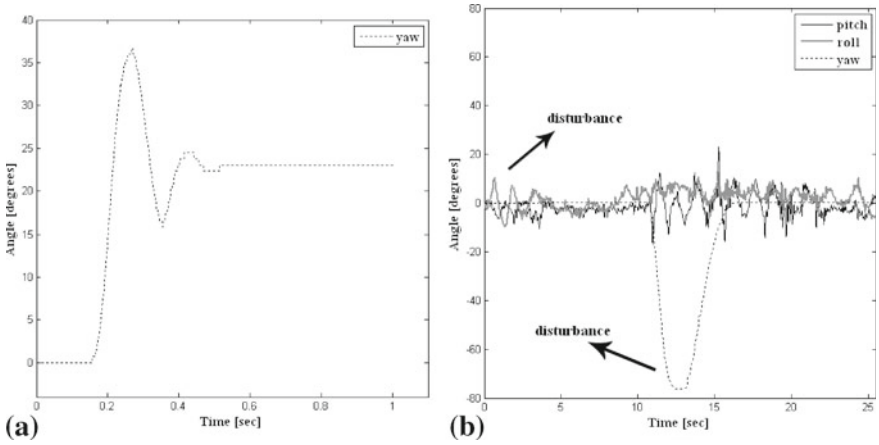

Figure 10. (**a**) Yaw response to a step command of 23 degrees. (**b**) Pitch, roll and yaw's control under random disturbances.

the yaw motion, sequential control is applied accordingly. That is, first, pitch-roll control is performed and it is ensured that pitch-roll compensation keeps the system under certain error in degrees figure 4. Then, yaw compensation is enabled to hold the system in certain yaw angle. Figure 9a. shows the response of the system to an initial condition of 3 degrees in roll angle and 12 degrees in pitch angle. System reaches its steady-state about ± 2 degrees, near-horizontal value, immediately. Since the employed inclination sensor is very sensitive to environmental noises, resulting vibrations need to be studied in future works. System response to, random, sudden disturbances is also tested as in figure 9b. A manual random disturbance is applied and vehicle returns to its horizontal position. Finally, when the pitch-roll error is under a certain degree and their coupling effect with the yaw axis is minimal, yaw control is enabled and 23 degrees of reference input is fed to the system in figure 10a. Because of the pre-compensation effects embedded on the control line reflecting the each motor's effect on yaw acceleration as in figure 5, response is fast and steady state value is very definite. In figure 10b, sequential control of all axes is illustrated. Quadrotor becomes stable when there is an initial error or random sudden disturbances. Figure 10b shows the responses of the system under random sudden disturbances when all axes controls are activated. First 5 seconds of figure 10b shows the control for pitch and roll when random sudden disturbances for only pitch and roll are applied to the quadrotor. From 10 to 20 seconds show the complete control of pitch, roll and yaw when random sudden disturbances for all pitch, roll and yaw are applied to system. The system compensates the error and become stable as can be seen from the figure 10b.

6. Conclusion

A stationary quadrotor with variable degree of freedom is studied to understand the mobility dependent control effectiveness. Since flight control algorithms are better to be studied on a real system for their usefulness, a stationary but functional air vehicle is preferred. Additionally, locking capability of different axes let the designer to observe the dynamic behaviour of the system under different controls for educational purposes. It is observed that yaw dynamics complicates the overall dynamics over pitch and roll dynamics of the quadrotor. However, reverse

effect is not present over yaw control. This effect is also illustrated in figure 5 that a larger value of PWM% duty cycle is needed in order to change the drag force for the same value of thrust force. Motor dynamics are not identical and affect system control in the first place. Because of similar reasons explained above, yaw control can compensate any disturbances (including non-identical motor dynamics) better than pitch-roll control. Yaw control and pitch-roll controllers are not similar because they do not have same sensitivity to varying control signals which is PWM % duty cycle. Yaw control needs larger values of control signal in PWM % duty cycle unit. Therefore, it is observed that two separate controllers designed for each pitch-roll and yaw axes result in a better performance, because fine-tuning of each axis has dissimilar requirements. It is also observed that sequential control of pitch-roll and yaw is more successful. When there is a term like 'yaw control is active if and only if pitch and roll error is under a defined value' in yaw controller's algorithm, the whole system response to random sudden disturbances becomes better. As a continuation of this study, extensive control applications employing locking capability of the system will be performed. Also, full spatial motion response of the system is to be experimented using the same or diverse nonlinear control algorithms.

Notations

b	[Ns^2]	Propeller thrust factor
d	[Nms^2]	Propeller drag factor
e	[rad]	Tracking error
$\dot{e}$	[rad/s]	Tracking error derivative
g_a	[ ]	Self tuning adjustment parameter
g_{de}	[ ]	Fuzzy adjustment parameter for error
g_e	[ ]	Fuzzy adjustment parameter for error derivative
I_{xx}	[Nms^2]	Quadrotor moment of inertia of around x-axis
I_{yy}	[Nms^2]	Quadrotor moment of inertia of around y-axis
I_{zz}	[Nms^2]	Quadrotor moment of inertia of around z-axis
J_{TP}	[Nms^2]	Total rotational moment of inertia around the propeller axis
k_d	[ ]	Derivative control constant
k_p	[ ]	Proportional control constant
l	[m]	Quadrotor wing length
m	[kg]	Mass of quadrotor
U	[ ]	Controller Output
U_1	[N]	Vertical thrust
U_2	[Nm]	Roll torque
U_3	[Nm]	Pitch torque
U_4	[Nm]	Yaw torque
U_{c1}	[ ]	Self tuning effect
U^{PD}	[ ]	Fuzzy PD Output
ϕ	[rad]	Angular position around x-axis
θ	[rad]	Angular position around y-axis
ψ	[rad]	Angular position around z-axis
Ω	[rad s^{-1}]	Overall propellers' speed
Ω_1	[rad s^{-1}]	Front propeller speed

Ω_2	[rad s^{-1}]	Right propeller speed
Ω_3	[rad s^{-1}]	Rear propeller speed
Ω_4	[rad s^{-1}]	Left propeller speed

References

Altug E, Ostrowski J P and Mahony R 2002 Control of a quadrotor helicopter using visual feedback, *IEEE International Conference on Robotics and Authomation, ICRA 2002*, Washington, DC

Amir M Y and Abbass V 2008 Modeling of Quadrotor Helicopter Dynamics, *International Conference on Smart Manufacturing Application*, 100–105

Baran E A, Hançer C, Çalıkoğlu E, Duman E, Çetinsoy E, Ünel M and Akşit M F 2008 An Experimental Setup Design for Unmanned Air Vehicles, *TOK'08 Automatic Control National Conference*, Istanbul, Turkey

Bouabdallah S, Murrieri P and Siegwart R 2004 Design and control of an indoor micro quadrotor, *IEEE International Conference on Robotics and Automation*, 4393–4398

Bresciani T 2008 *Modelling, Identification and Control of a Quadrotor Helicopter*, Adv: Daniele Caltabiano, Master's Thesis, Lund University

Castillo P, Lozano R and Dzul A 2005 Stabilization of a Mini Rotorcraft with Four Rotors, *IEEE Control Systems Magazine*, 45–55

Chen M and Huzmezan M 2003 A Simulation Model and H^{∞} Loop shaping Control of a Quad Rotor Unmanned Air Vehicle, *Proceedings of IASTED International Conference on Modelling, Simulation and Optimization*, 320–325

Dierks T and Jagannathan S 2010 Output Feedback Control of a Quadrotor UAV Using Neural Networks, *IEEE Transactions on Neural Networks*, 21(1):50–66

Efe M O 2007 Dynamic Model and PD controller-based path control of a Quadrocopter *TOK'07*, *Automatic Control National Conference*, Istanbul, Turkey

Engin S N, Kuvulmaz J and Ömürlü V E 2004 Fuzzy control of an ANFIS model representing a nonlinear liquid-level system, *Neural Computing and Applications*, 13(3):202–210

Fang Z, Zhi Z, Jun L and Jian W 2008 Feedback Linearization and Continuous Sliding Mode Control for a Quadrotor UAV, *27th Chinese Control Conference*, CCC

Han-Xiong L and Gatland H B 1996 Conventional Fuzzy Control and its enhancement, *IEEE Transactions on Systems, Man and Cybernetics, Part B: Cybernetics*, 26(5):791–797

Hoffmann G, Rajnarayan D G and Waslander S L 2004 The Stanford Testbed Of Autonomous Rotorcraft For Multi Agent Control (Starmac), *Digital Avionics Systems Conference*, Salt Lake City, UT

Kim J, Kang M S and Park S 2010 Accurate Modeling and Robust Hovering Control of a Quadrotor VTOL Aircraft, *J. Intelligent and Robotic Syst.*, 57(1):9–26

Mian A A and Daobo W 2008 Modeling and Backstepping-based Nonlinear Control Strategy for a 6 DOF Quadrotor Helicopter, *Chinese Journal of Aeronautics*, 21(3):261–268

Mokhtari A, Benallegue A and Daachi B 2006 Robust Feedback Linearization and GH^{∞} Controller for a Quadrotor Unmanned Aerial Vehicle, *J. Electric. Eng.*, 57(1):20–27

Mudi R K and Pal N R 1999 A robust selt-tuning scheme for PI and PD type fuzzy controllers, *IEEE Transactions on Fuzzy Systems*, 7(1):2–16

Ömürlü V E, Kirli A, Büyükşahin U, Engin S N and Kurtoglu S 2011 A stationary, variable DOF flight control system for an unmanned quadrocopter, *Turkey J. Elec. Eng. Comp. Sci.* 19(6):891–899

Patel C A, Rao S K and Driessen B J 2006 A testbed for mini quadrotor unmanned aerial vehicle with protective shroud, *2nd Annual Symposium on Graduate Research and Scholarly Projects*, Wichita State University, Wichita

Pongpaibul B 2001 *Experimental Flying Autonomous Vehicle*, Advs: Dr. Victor Becerra and Dr. William Browne, Thesis, Reading University

Pounds P, Mahony R, Hynes P and Roberts J 2002 Design of a Four-Rotor Aerial Robot, *Australasian Conference on Robotics and Automation*, Auckland, New Zealand

Raffo G V, Ortega M G and Rubio F R 2010 An integral predictive/nonlinear H^{∞} control structure for a quadrotor helicopter, *Automatica*, 46(1):29–39

Tayebi A and McGilvray S 2006 Attitude stabilization of a VTOL Quadrotor Aircraft, *IEEE Trans. Control Syst. Technol.*, 14(3):562–571